

On the zonal distribution of South Atlantic Central Water (SACW) along a section off Cape Blanc, Northwest Africa

South Atlantic Central Water
Energy distribution
Cape Blanc

Eau Centrale de l'Atlantique Sud
Répartition de l'énergie
Cap Blanc

Eberhard HAGEN, Rudolf SCHEMAINDA
Academy of Sciences of the German Democratic Republic,
Institute of Marine Research, DDR-2530 Rostock-Warnemünde, GDR.

Received 6/8/85, in revised form 9/6/86, accepted 21/8/86.

ABSTRACT

The hypothesis of isopycnal mixing was used in order to calculate the percentages of South Atlantic Central Water (SACW) in proportion to North Atlantic Central Water (NACW) in the intermediate layer between the density surfaces of $\sigma_t = 26.5$ and $\sigma_t = 27.2$ along a zonal section at $20^{\circ}10'N$.

In this profile the SACW distribution was "conserved" within an offshore distance of about 370 km from the African coast during two observation periods with a time lag of ten months. The SACW distribution along the section follows from the zonal energy structure of the geostrophic meridional flow within this layer.

It is concluded that the intermediate geostrophic meridional motions are adjusted to the local profile of the continental slope $H(x)$.

For this reason, the condition $(f/H)(dH/dx)/\beta > 1$ delimits a nearslope zone where the "conservation" of the distribution of energy and of SACW was observed.

Oceanol. Acta, 1987. Proceedings International Symposium on Equatorial Vertical Motion, Paris, 6-10 May 1985, 61-70.

RÉSUMÉ

Sur la répartition zonale de l'Eau Centrale de l'Atlantique Sud (ECAS) le long d'une section au large du Cap Blanc, Afrique du Nord-Ouest

L'hypothèse du mélange isopycne a été utilisée pour calculer les proportions de l'Eau Centrale de l'Atlantique Sud (ECAS) et de l'Eau Centrale de l'Atlantique Nord (ECAN) dans la couche intermédiaire située entre les surfaces de densité $\sigma_t = 26,5$ et $\sigma_t = 27,2$, le long d'une coupe à la latitude de $20^{\circ}10'N$.

Dans cette coupe, la répartition de l'Eau Centrale de l'Atlantique Sud a été « conservée » pendant deux campagnes de mesures espacées de dix mois à l'intérieur d'une zone s'étendant de la côte africaine à environ 370 km au large.

La répartition de l'Eau Centrale de l'Atlantique Sud le long de la coupe résulte de la structure de l'énergie du courant méridien géostrophique à l'intérieur de cette couche.

En conclusion, les mouvements méridiens géostrophiques intermédiaires intervenant dans cette couche s'ajustent au profil local de la pente continentale $H(x)$.

Pour cette raison, la condition $(f/H)(dH/dx)/\beta > 1$ délimite une zone proche de la pente continentale à l'intérieur de laquelle on a observé une « conservation » de la répartition de l'énergie et du pourcentage de l'Eau Centrale de l'Atlantique Sud.

Oceanol. Acta, 1987. Proceedings International Symposium on Equatorial Vertical Motion, Paris, 6-10 May 1985, 61-70.

INTRODUCTION

Upwelling is a well-known phenomenon in the areas of eastern boundary currents of the basin-scale circulation off the west coasts of continents, especially in subtropical and tropical regions with permanent tradés.

The nearshore zone is indicated inter alia by motions trapped on the scale of the baroclinic deformation radius R (Yoshida, 1967).

Many observations indicate that coastal upwelling extends further offshore than R . Such broad extension of a "disturbed nearshore zone" requires an explanation in relation to the fact that coastal upwelling is an immanent process within the whole system of eastern boundary currents. Following Philander and Yoon (1982) we accept here that annual and/or semiannual Rossby waves determine the offshore scale of upwelling and that the resulting offshore scale is locally modified by the zonal profile of the continental shelf slope.

We base our argument on CTD-observations along a zonal section extending 1 000 km from the northwest African coast at the latitude of $21^{\circ}10'N$ off Cape Blanc.

A coordinate system rotating with the earth is used with the x-axis onshore, y-axis northward, and z-axis upward.

DATA BASE AND PROCESSING

The data used result from two expeditions of the r/v "A. v. Humboldt" of the Academy of Sciences of the GDR, carried out during March/April 1983 and

February/March 1984 with a time lag of about 10 months (see Fig. 1 for station positions). At each hydrographic station the pressure, temperature, conductivity, and oxygen content were continuously monitored by means of the measuring system "OM-75", lowered from the sea surface down to the pressure level of 1 500 dbar. This oceanographic measuring system was described in detail by Möckel (1980); the validation procedure used was discussed by Lass *et al.* (1983).

Station spacing was 10 nautical miles over the shelf but commonly 20 nm further offshore.

The temperature sensor was always controlled by two reversing thermometers at each station in different water depths. Corresponding comparisons were carried out for salinity measurements between the system sensor and salinometer measurements. All necessary corrections were taken into account.

The possibility of errors in the data sampled along the section, produced by the mixing of time-space scales and generally ascribed to one-ship measurements, was not ruled out.

CENTRAL WATERS AND ISOPYCNAL MIXING

The central water masses of the oceans are defined by a nearly linear temperature-salinity (TS)-relationship between characteristic peak values, according to the classical definition presented by Sverdrup *et al.* (1952). These water masses occur in the permanent pycnocline between depths of 100 and 600 m in subtropical and tropical oceans. We can distinguish the North Atlantic Central Water (NACW) from the South Atlantic Central Water (SACW) in the area

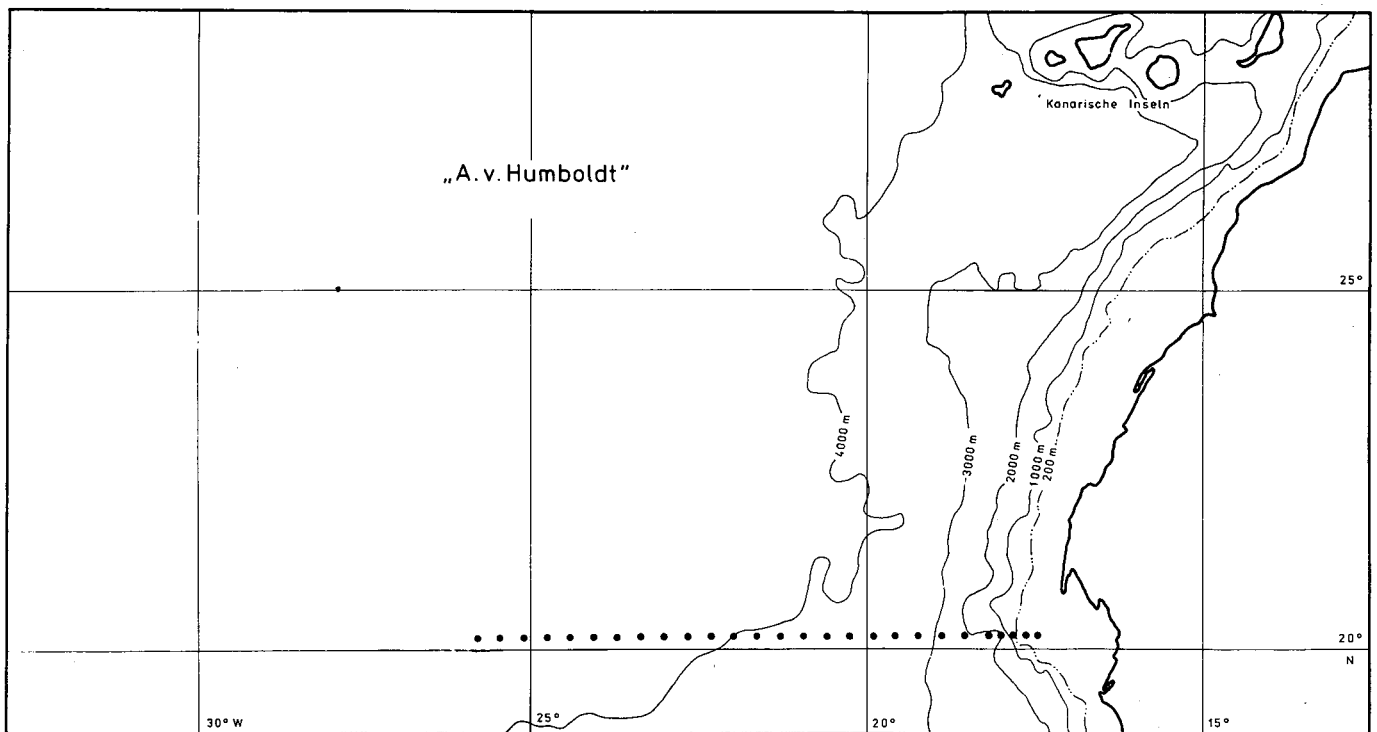


Figure 1

Station positions over a rough bottom topography along the zonal section which was treated by R/V "A. v. Humboldt" at latitude $20^{\circ}10'N$ during April 1983 and February 1984.

under consideration. The TS-characteristics of both central waters show regional deviations from the straight lines of definition. For instance, Tomczak and Hughes (1980) have used special definitions in order to study the mixing processes between NACW and SACW in the upwelling area off northwest Africa. We do not, however, believe such an approach to be the best way since the resulting water analyses are regionally fixed. Such a special investigation certainly yields important information on local mixing processes, but the results are not readily comparable with observations from neighbouring regions of the same upwelling area.

The extensive TS-data of the World Oceanographic Data Center were carefully analysed by Willenbrink (1982) with respect to the definition of central waters in the area between latitudes 8°N and 41°N and longitudes 8°W and 35°W. Because the resulting peak values of NACW and SACW harmonize well with the classical definition given by Sverdrup, we shall use a definition of central waters in the following form :

	upper limit	lower limit
NACW	T = 17.5°C S = 36.4×10^{-3}	T = 8.0°C S = 35.1×10^{-3}
SACW	T = 16.0°C S = 35.65×10^{-3}	T = 8.0°C S = 34.7×10^{-3}

According to Kirwan (1983) the isopycnal mixing analysis correctly describes the mixing between central waters marked by any linear TS-relation.

Furthermore, Tomczak (1981 *a* ; *b*) proposed a multi-parameter analysis including mixing of different nutrients additionally. Using this method Fraga *et al.* (1985) calculated nutrient contents which we can expect for "pure" SACW and "pure" NACW.

SACW is more rich in nutrients than NACW. But it is important to note that in contrast to temperature and salinity, which are definitely conservative parameters, phosphate, nitrate, and silicate are influenced by the biochemical cycle within surface and subsurface layers alike.

Because of such methodic uncertainties, and in the absence of a careful estimation of the influences

produced in this way, we shall desist from the application of multi-parameter technique in the present case. The following estimations of relative percentages of the mixing waters between SACW and NACW are made strictly on the basis of isopycnal mixing in subsurface layers. It has been shown by Fraga (1974), Tomczak (1978), and several other oceanographers that the upwelled water originates from different sources in the investigation area. The properties of upwelled water are mainly determined by NACW in regions located north of Cape Blanc (21°N) while the influence of SACW on the upwelling waters increases with decreasing latitude. Consequently, a permanent front zone which separates the NACW and SACW is formed at depths between 100 and 600 m, nearly at the latitude of Cape Blanc [see, for instance, Manriquez and Fraga, (1962)].

This intermediate frontal zone is indicated by drastic gradients of different parameters meridionally. For example, Barton (1985) reported salinity gradients of $1.10^{-3}/10$ km within the front. The steadiness of the front zone can only be made possible by a continuous injection of SACW and NACW into this zone of discontinuity by undercurrents running at depths between 100 m and at least 400 m off the shelf break. The upwelling undercurrent (UUC) is a dynamic part of the entire system of eastern boundary currents and reacts well on the Ekman offshore drift in the 30 m top layer (see Fig. 2), but also on remote forcings. For times much longer than about a half-year, the UUC follows the meridional pressure gradients which are well in balance with the alongshore component of the wind stress at the sea surface, compare Philander and Yoon (1982) for more details. In our view, the poleward UUC is also radiated to the west in form of annual forced Rossby waves as the equatorward current in the top layer.

Caused by the seasonal shifting of northeast trades, we can only observe a relative small region with permanent coastal upwelling during the whole year according to Schemainda *et al.* (1975), Wooster *et al.* (1976), and Speth *et al.* (1978). This region is meridionally bounded between 20°N in the south and 25°N in the north. In other words, the front zone between SACW and NACW lies in the area of permanent upwelling. On its way into this boundary region, the SACW percentage of the UUC rapidly decreases down to values between 50 and 20 or 10 %.

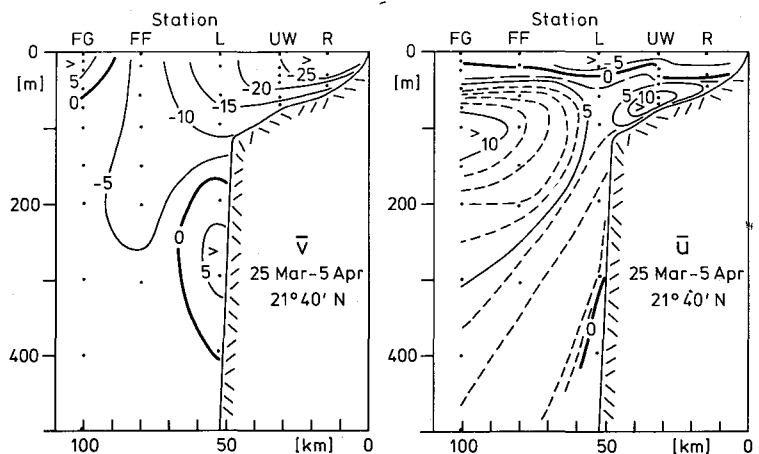


Figure 2

Mean structures of the onshore component \bar{u} (negative to west) and the corresponding alongshore component \bar{v} (negative to south) observed by an array of current meters during the experiment Joint-I in 1974 (from Mittelstaedt *et al.* (1975)).

ALONGSHORE WIND

The classical picture of coastal upwelling calls for a brief presentation of the offshore structure of the alongshore wind component.

For instance, it was shown by Speth *et al.* (1978) that the north-south component of northeast trades is basically geostrophic in the investigation area.

Because the signal-noise relationship is more favourable for measurements of air pressure than for actual wind observations, we shall limit our interest to the offshore structure of air pressure p^a . The zonal gradients of p^a determine the geostrophic part of the local north-south winds.

Figure 3 indicates a dominating southward wind from the shore up to a distance of about 400 km. Furthermore, the mean zonal slope of p^a is nearly constant in this boundary zone while the gradients of p^a disappear further offshore.

The observations presented in Figure 3 agree well with the corresponding zonal structures of the meridional winds obtained by Krauss and Wuebber (1982). Their Figure 5 shows that the zonal shear of the meridional wind stress disappears in the nearshore region of about 400 km along the African coast between 25 and 27°N during the whole year. These facts permit us to surmise that the offshore pattern of alongshore winds can make a significant contribution to the formation of a nearshore boundary zone.

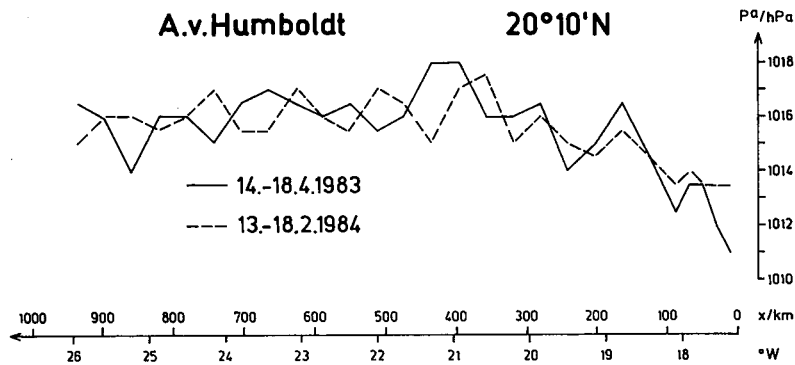


Figure 3

Zonal distribution of the air pressure p^a as indicator for geostrophic meridional winds along the section shown in Figure 1 for both observation periods (the offshore distance starts at the 20 m depth of the bottom topography).

SACW DISTRIBUTION

Two actual sections of zonal SACW percentages obtained by the assumption of isopycnal mixing are presented in Figure 4. The observations were repeated with a time lag of about ten months during the upwelling season.

The core of the UUC is indicated by concentrations of more than 70 % of SACW at depths between 100 and 200 m off the continental slope. Its offshore extension is no more than about 30/40 km and reflects the influence of R on the inner motions. A second SACW core was observed between 300 and 500 m. Both cells of SACW enrichment are separated by a strip of poor percentages, lower than 20 % of SACW. Moreover, a third core was indicated with more than 40 % of SACW at shallower depths between 150 and 200 m on the offshore flank of the nearshore zone at a distance of about 400 km from the shore.

Generally speaking, the described structures were "conserved" within the 370/400 km boundary zone. The "freezing" of such characteristic SACW pattern underlines the hypothesis that permanent SACW cores are an adequate tracer for "steady state" currents which transport the properties of SACW from the south into the region off Cape Blanc. Contrary to the established structures of SACW

distribution in the 370/400 km nearshore zone during both observation periods, it is also demonstrated by Figure 4 that sporadic SACW patterns dominate further offshore, at least westward of 21°30'W, where other physics enter the motion dynamics. The SACW cores shown in Figure 4 are well documented by analogical patterns for the minimum of oxygen content and for the maxima of corresponding phosphate in Figure 5.

INTERMEDIATE GEOSTROPHIC MERIDIONAL FLOW

An example for measured currents was shown in Figure 2. These observations were carried out at the latitude of 21°40'N during a late upwelling season.

The UUC core is given *inter alia* by averaged speeds larger than $5 \cdot 10^{-2} \text{ m s}^{-1}$ at depths of about 300 m. Its total offshore extent is roughly given by the distance of 20 km from the continental shelf slope.

In order to demonstrate the geostrophic character of the UUC, Figure 6 shows the meridional components \bar{v}_r estimated at the level of 300 m relative to the reference depth of 700 m along the section.

Generally, the conformity between the SACW distribution of Figure 4 and the geostrophic north flow of

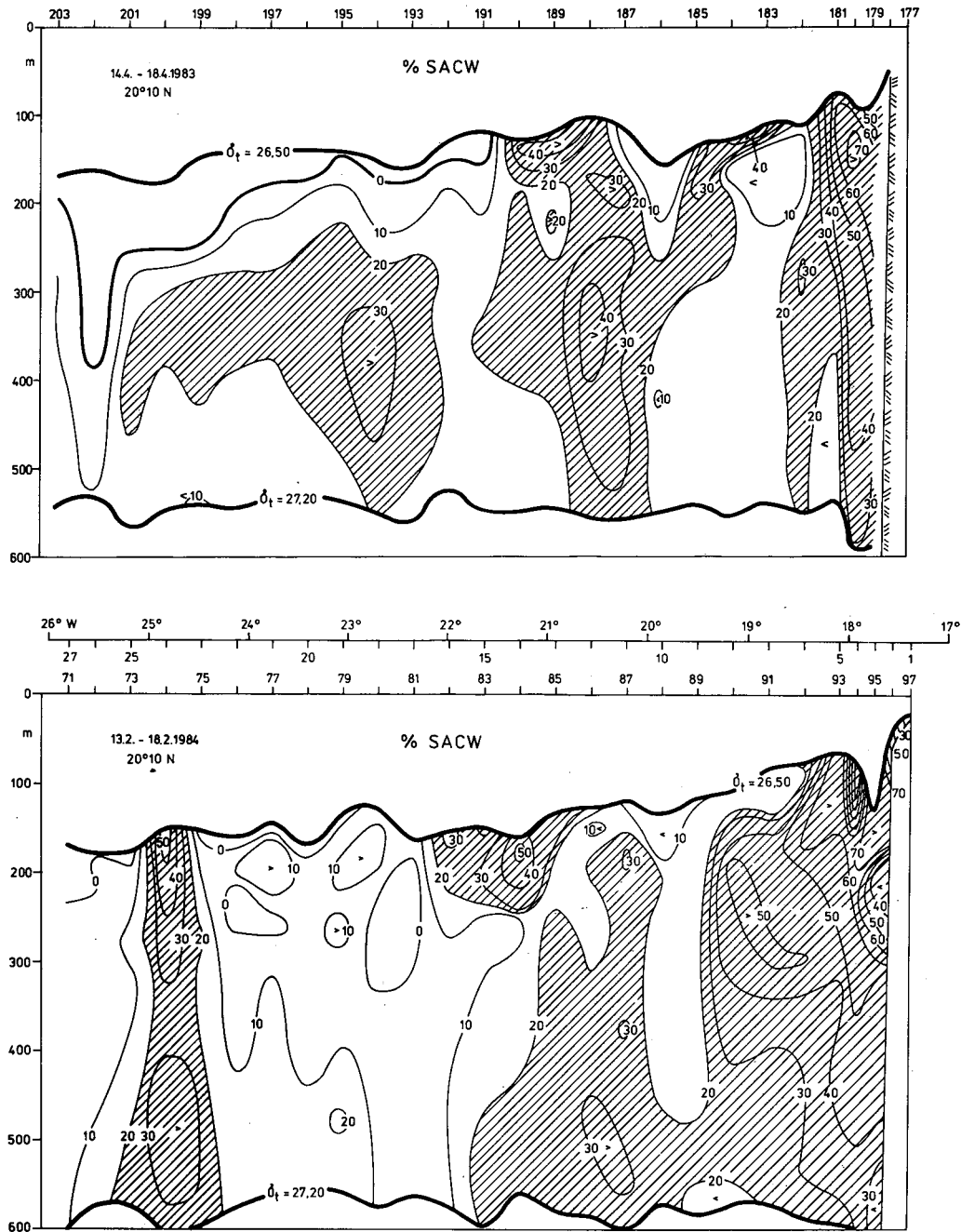


Figure 4

Percentages of South Atlantic Central Water (SACW) (30% of SACW correspond to 70% of North Atlantic Water (NACW)) between selected density surfaces. The actual station number, the

numbered stations (1-27), and the longitude are separately indicated at the abscissa.

Figure 6 is only poor. This absence of sufficient agreement is caused, among other things, by the motions at the reference level. Nevertheless, the nearshore core of SACW is clearly in correspondence with the northward currents at 300 m for both cases. The poleward flow is confined on the offshore scale of about 50 km, that is the order of R . However, the second SACW core is poorly reflected by a corresponding northward current at this level. We find a weak component to north between the distances of 400 and 350 km (between 20 and 20°30'W) while the sign of \bar{v}_r alternates in areas located further offshore.

It is interesting to note that a southward motion

occurs on the seaward flank of the UUC. The location of its peak values agree well with the zone of low percentages of SACW. If we take into consideration the mean methodic errors of about $\pm 7.10^{-2} \text{ m s}^{-1}$, then we can only conclude from Figure 6 that the geostrophic part of the UUC is nearly trapped on the scale of R at the level of 300 m with respect to the reference level of 700 m.

Of course, the choice of the reference depth was arbitrarily intended. We shall attempt to describe the zonal structures of the layer thickness $D(x)$ between the density surfaces $\sigma_t = 26.5$ and $\sigma_t = 27.2$, because the SACW is mainly observed within this layer.

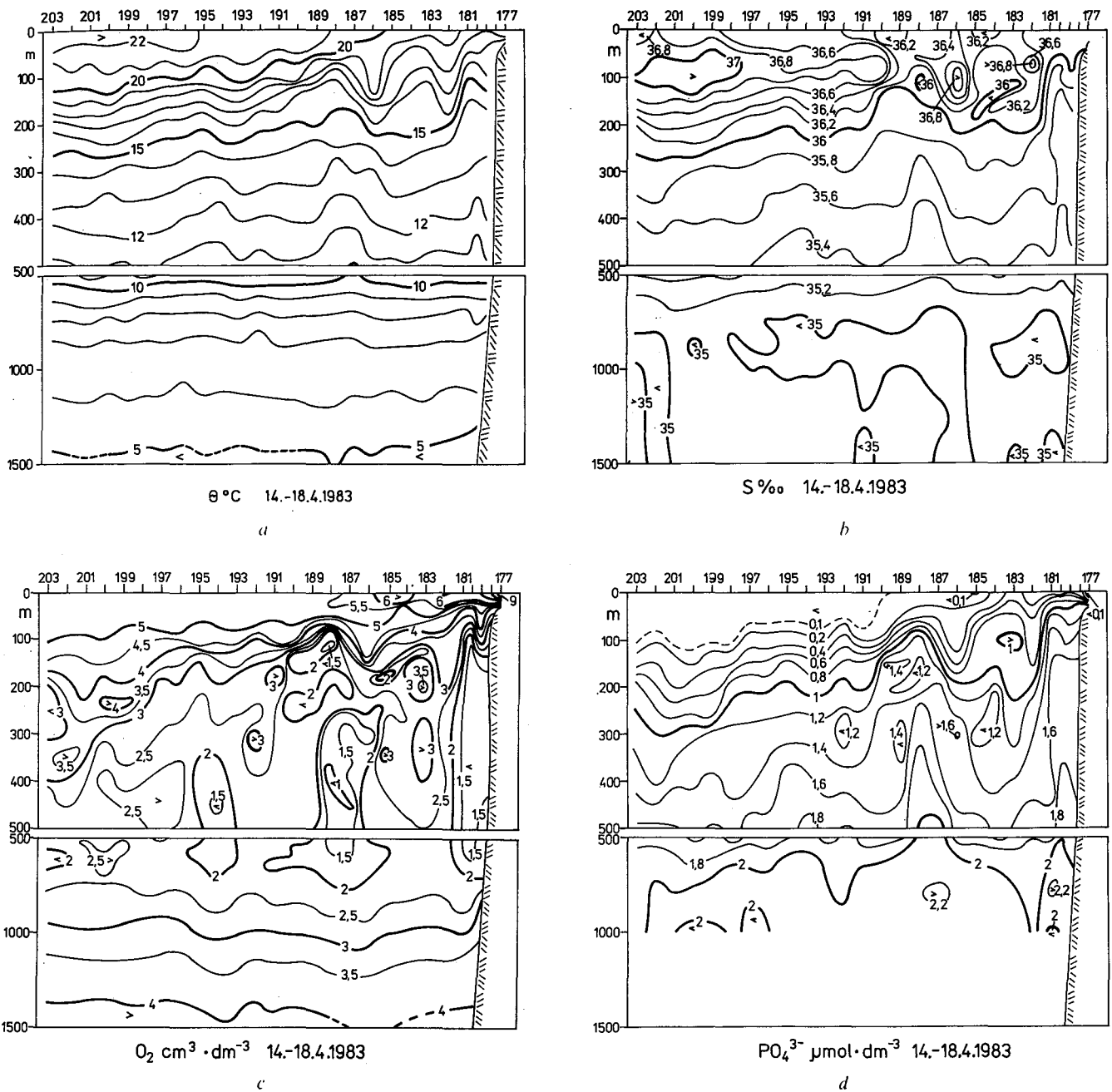


Figure 5
Zonal sections of oxygen O_2 , and phosphate PO_4^{3-} observed south of Cape Blanc in 1983 (note that the vertical scale is changed below 500 m and that the "disturbed boundary zone" is observed between stations 177 and 190).

500 m and that the "disturbed boundary zone" is observed between stations 177 and 190).

INTERMEDIATE ENERGY STRUCTURES

In the following, we assume that the motions are geostrophically adjusted in the intermediate layer between density surfaces of $\sigma_t = 26.5$ and $\sigma_t = 27.2$. The layer thickness enclosed is $D(x)$.

From the thermal wind equation, it follows that the vertical difference of the meridional flow averaged over this layer is given by $v = \Delta v = (g'/f)(\Delta D/\Delta x)$. Here, v denotes the relative velocity at the level of the upper surface with respect to the vanishing motion at the lower density surface. The reduced gravity is $g' = -g(\Delta\rho/\rho_0)$ with the acceleration of gravity g , the density difference $\Delta\rho$, and the constant reference

density ρ_0 . The Coriolis parameter is f at the latitude of $20^\circ 10' N$. The station separation is Δx while ΔD is the difference of layer thickness between neighbouring stations. Averages resulting from the entire section are marked by an over-bar. The contribution of v_i to the local level of kinetic energy was estimated by $E_k = (v_j - \bar{v})^2$ at i -positions between the stations while the contribution of potential energy was estimated by $E_p = g'(D'_j/\bar{D})$ at the j -station positions along the section. The local anomaly of the layer thickness is given by $D'_j = (D_j - \bar{D})$.

According to the assertions noted above, we expect a conserved zonal structure of E_k and E_p in the nearshore zone with a range of about 370/400 km

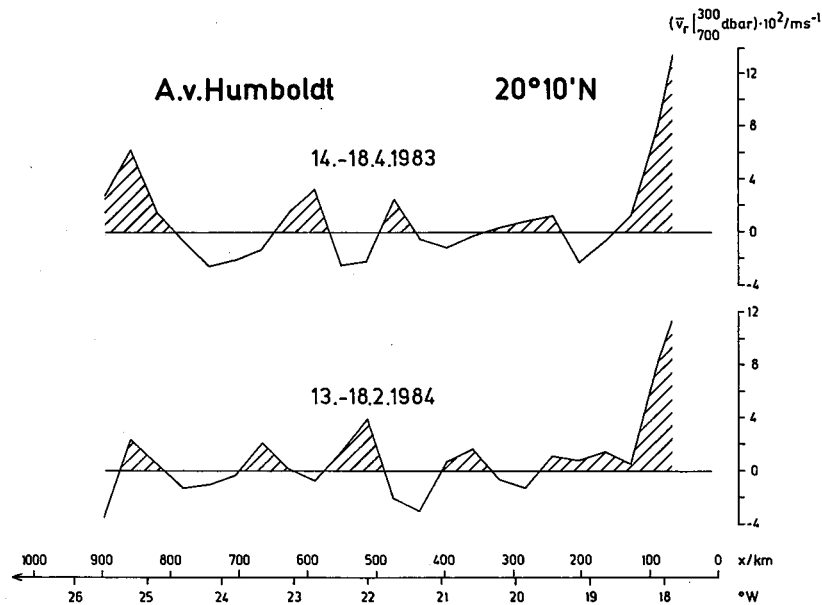


Figure 6

Zonal structures of the geostrophic meridional velocity \bar{v}_r (negative to south) at the level of 300 dbar relative to 700 dbar estimated by the dynamical method with a mean methodic error of about $\pm 7 \cdot 10^{-2} \text{ms}^{-1}$ during both observation periods.

from shore. In fact, Figure 7 shows those conditions up to a distance of about 370 km (21°W) from the coast. Furthermore, the relationship β_T/β obtained from the local shelf profile $H(x)$ is represented with $\beta_T = (f/H) \cdot (dH/dx)$ and $\beta = 2 \cdot 10^{-11} \text{m}^{-1} \text{s}^{-1}$. The zone with dominating topographic influences is hatched. This bottom controlled zone is marked by $\beta_T > \beta$. A confuse middle strip of about 300 km is indicated by the condition $\beta_T \approx \beta$ while the region further offshore is marked by $\beta_T < \beta$.

Thus, the total section is zonally divided into three zones characterized by different conditions with respect to barotropic motions.

Using the CTD-data published by Halpern and Holbrook (1977) which result from the experiment Joint-I at latitude 21°40'N during March/April 1974, we have estimated the zone marked by $\beta_T/\beta > 1$ to extend to about 200 km from the shore, although the winds observed were without a significant boundary in the offshore direction.

We believe these observations to underline the hypothesis proposed, since the vertical sections of temperature, salinity, and density show astonishing agreement with the structures presented in Figure 5, especially between stations 177 and 190 at depths between 50 m and at least 300 m [compare also the sections shown by Jones (1972) and Barton (1982)]. In our view, Figure 2 shows typical current structures in intermediate depths for the zone off the shelf slope.

We also judge that the decreasing offshore scale by the factor of about two is essentially caused by the narrow width of the continental shelf at 21°40'N, in comparison with the relatively broad continental shelf at 20°10'N which is present south of Cape Blanc in the form of the Banc d'Arguin (*cf.* Fig. 1).

DISCUSSION

Our understanding of upwelling dynamics is being advanced at present by many analytical and numerical models as well as by field observations. It is commonly accepted that upwelling is a time-dependent, non-linear, three-dimensional, boundary layer process, stochastic in nature. Therefore, the recent upwelling picture developed by modellers and seagoing oceanographers is highly complicated not only in different space, but also in different time-scales.

Nevertheless, comparisons between current structures derived from models, moored current meters, drifters and mass field analyses show some uniformity with respect to the importance of the deformation radius R . For the investigation area we can expect $R = 42$ km for mean conditions according to Emery *et al.* (1984). The coldest nutrient-rich water is observed at the surface within the R -scale off Cape Blanc during the whole year. Examples from observations are discussed by Schemainda *et al.* (1975), Mittelstaedt *et al.* (1975) and many other authors. But we can relate other examples from the literature too. The influence of upwelled water appears at distances of more than 100 km from the shore line in different upwelling areas, as was demonstrated, for instance, by Defant (1936) and Smed (1982). Furthermore, we know that the effect of Ekman pumping produced by the curl of wind stress in the offshore area is well correlated with the nearshore current system (Hickey, 1979). In other words, dynamic forcing conditions, far from the zone of investigation, also influence coastal upwelling. On the other hand, the typical space scale of northeast trades is much larger than the effect of upwelling directed in the offshore direction. Therefore, we can sum up that the upwelling phenomenon

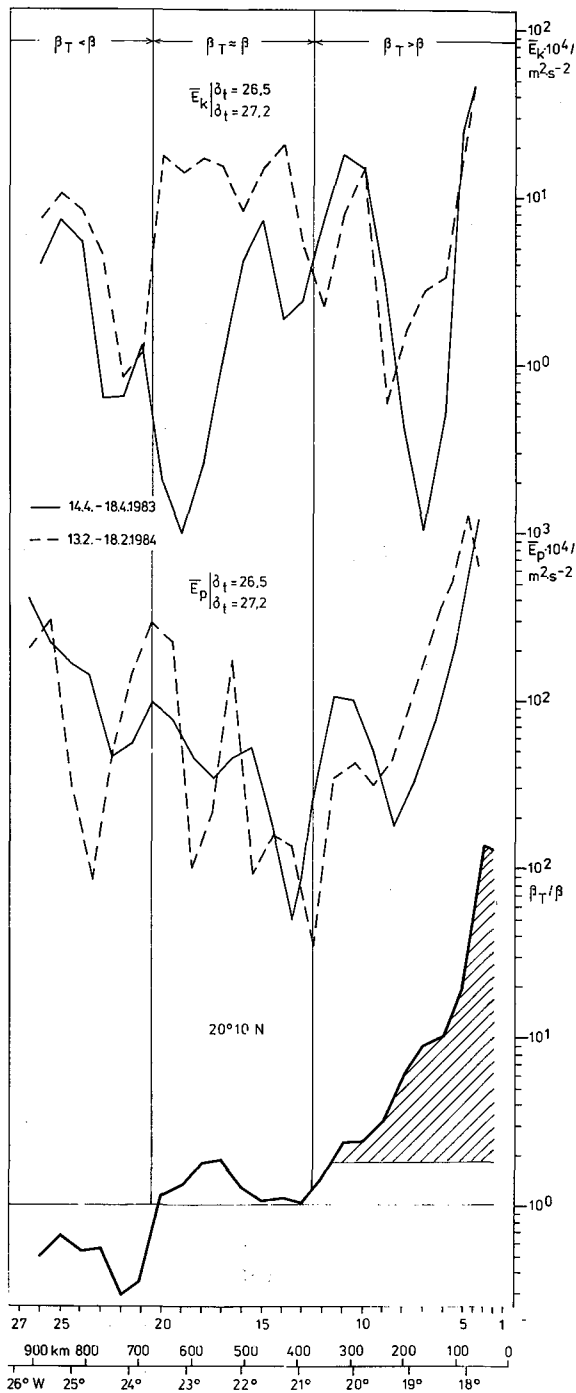


Figure 7
 Zonal structures of the relationship β_T/β determined from $\beta = 2 \cdot 10^{-11} \text{ m}^{-1} \text{ s}^{-1}$ and the local profile of the continental shelf slope $H(x)$ (the topographic controlled zone marked by $\beta_T > \beta$ is hatched) in comparison with structures of the potential energy E_p and the corresponding kinetic energy E_k of the intermediate meridional flow, geostrophic in nature, between the density surfaces of $\sigma_t = 26.5$ and $\sigma_t = 27.2$ (independent of an arbitrary reference level) where the spreading of SACW is mainly observed.

is a result of the joint action of different physical processes which occur in diverse space-time scales. According to the scenario compiled by Philander and Yoon (1982) it is an important fact that the R-scale is replaced by the distance which Rossby waves travel westwards from the nearshore zone after a critical time. The parameters necessary to check this larger distance are the R-scale and the forcing period of

wind fluctuation. By this reckoning, the offshore scale of a "disturbed coastal region" depends on the time scale of typical fluctuations of trades. In the investigation area, the annual and/or semiannual period is the most energy-rich wind fluctuation, compare for instance Michelchen (1981). According to the scenario proposed, we receive with $R = 42 \text{ km}$ and an annual forcing the critical time of 173 days, roughly a half-year. A complex system of northward and southward currents appears after this time. Coastal currents are radiated by Rossby waves in the offshore direction.

For our example, we receive a westward propagation of about 0.02 m s^{-1} for first-mode waves. This value is sufficiently in accordance with corresponding estimations by Delecluse (1983). Furthermore, the offshore distance results as zonal wavelength from the speed of Rossby dispersion and the annual forcing period. In summary, we receive a distance of about 630 km for annual and 315 km for semiannual forced Rossby waves. Such offshore distances are in good harmony with the extension of the influence of upwellings on hydrographic field distributions observed at the sea surface in the area under consideration.

For very low frequencies, the local time variation of relative vorticity of the current field is well expressed by the dynamics of Rossby waves. It was shown in a classical publication by Veronis (1966) that the effect of bottom topography is very important in generating low-frequency waves, sometimes more important than the β -effect for relatively small changes in water depth, especially the changing water depth parallel to the shore. On the other hand, we know that topographic gradients directed in the across-shelf direction dominate on corresponding alongshore gradients in the study area off Cape Blanc. From the conservation of potential vorticity of depth-independent motions, we receive two essential influences which can locally act in concert to balance the time-changing of relative vorticity. The first results from changes of the Coriolis frequency f with the latitude and it is noted by β .

The second is found to be $\beta_T = (f/H) (dH/dx)$ by the assumption $|dH/dx| \gg |dH/dy|$ with the water depth H .

The "shore line" roughly coincides with the 20 m isobath of the bottom topography. The ratio β_T/β is the relationship between topographic and planetary influences of barotropic motions over the continental shelf slope.

Following Gill and Niiler (1973), we wish to speculate that the variations of sea level are essentially determined by the steric changes of the heat content of the whole water column.

For instance, it was shown by Verstraete and Picaut (1983) that the monthly response of the intermediate mass field is well correlated with barotropic sea level variations in the Gulf of Guinea. We also anticipate those correlations in the area under consideration.

Commonly, the baroclinic flow is subject to the bottom topography in two ways; directly through the action of the bottom slope on the currents in the deepest layers and indirectly through interaction with barotropic motions over the whole water column.

Considering that the response of the main body of the water column to a large-scale forcing by winds is "quasi-barotropic", we take into the consideration

that the ratio β_T/β essentially influences the nearshore dynamics of motion.

As regards annual and/or semiannual forced Rossby waves, we suggest that these start from the slope zone marked by the condition $\beta_T \approx \beta$, because planetary vorticity determines the motion seaward of this zone while the topographic controlled divergence produced over the continental shelf slope shoreward forms a nearshore zone for the part of the large-scale circulation which is more "steady state" in nature. Of course, we have to consider deviations from the mean flow signal in this nearshore zone. According to Suginohara (1982), such fluctuations have typical time scales of a few weeks, and are formed by topographic trapped waves. Freely drifting geostrophic eddies were reported by Tomczak and Hughes (1980) with a typical life time of several weeks. Baroclinic wave-like processes and eddy-like features show time scales which are much larger than the observation duration of about five days needed for measurements along the entire zonal section. Therefore, we think that such phenomena are locally "fixed" during the observation time and that we can roughly exclude unnecessary errors in the presented data.

CONCLUSIONS

It is probable that the total offshore extent of ecosystem "upwelling" is not only determined by pure wind-produced dynamics on the shelf but also by the whole system of eastern boundary currents which is mainly characterized by meridional motions in intermediate layers off the continental shelf slope. The current fluctuations of this system show a broad range of space and time scales.

In summary, we can consider four important contributions, resulting from different processes, to the production of a "disturbed" flow and mass field in the nearshore zone:

- the offshore scale of trapped waves travelling to the north in the subinertial frequency range along the wave guide of the continental shelf slope;
- the replacing of the baroclinic radius of deformation by the offshore scale of annual forced Rossby

waves travelling to the west after a critical time of about a half-year to generate a complex system of northward and southward currents in the zone of interest;

- the topographic scale controlled by the ratio β_T/β with respect to the part of the "steady state" meridional flow within intermediate layers of subsurface currents (or with respect to internal, meridional pressure gradients which are mainly balanced by the meridional winds and are also adapted to the bottom profile);

- the offshore scale of the southward component of north-east trades which acts as a "boundary" for the generation of the offshore transport in the top layer.

It should also be pointed out that those processes act in concert. The subsurface currents are permanent branches of this complex system of boundary currents. Any meridional flow-branch transports either SACW from south to north or NACW from north to south. Although the upwelling undercurrent (UUC) reacts well on far forcings it is locally adapted to the continental slope. It has become apparent that the zonal structure of baroclinic motions is divided into three regions by the ratio of topographic to planetary influences for barotropic motions. The nearslope zone is marked by $\beta_T > \beta$. This region extends to a distance of about 370 km from the shore in the study area off Cape Blanc. It follows a confuse middle zone marked by the conditions $\beta_T \approx \beta$ between distances of 370 and 670 km while the offshore zone is indicated by $\beta_T < \beta$.

Not only further investigations by extensive zonal sections but also current measurements across the continental shelf slope with a duration up to a year are required in order to understand those dynamics in greater detail, especially in order to clarify the conditions for the generation of typical zonal structures of SACW and the offshore extent of the marine ecosystem "coastal upwelling" embedded in the entire system of eastern boundary currents.

Acknowledgements

We wish to thank the reviewers of the manuscript for critical and constructional comments, and to express our gratitude for the invitation to the International Symposium by Dr. D. Halpern and Dr. R. Barber.

REFERENCES

- Barton E. D., 1982. Medium-scale water-mass structure near Cape Corveiro, Northwest Africa, in March 1974, Rapp. P.-V. Réunion. Cons. Int. Explor. Mer, **180**, 65-72.
- Barton E. D., 1985. Structure and variability of central water mass front off Cabo Blanco, October 1981-April 1982, in: *International Symposium on the most important Upwelling Areas off Western Africa (Cape Blanc and Benguela)*, edited by C. Bas, R. Margalef and P. Rubies, Instituto de Investigaciones Pesqueras, Vol. I, Barcelona, 49-61.
- Defant A., 1936. Das Kaltwasserauftriebsgebiet vor der Küste Südwestafrikas. Länderkundliche Studien (Festschrift W. Krebs), Stuttgart, 52-66.
- Delecluse P., 1983. Coastal effects on upwelling, in: *Hydrodynamics of the Equatorial Ocean*, edited by J.C.J. Nihoul, Elsevier Scientific Publ. Comp., 259-279.
- Emery W. J., Lee W. G., Magaard L., 1984. Geographic and seasonal distribution of Brunt-Väisälä frequency and Rossby radii in the North Pacific and North Atlantic, *J. Phys. Oceanogr.*, **14**, 294-317.
- Fraga F., 1974. Distribution des masses d'eau dans l'upwelling de Mauritanie, *Tethys*, **6**, 5-10.
- Fraga F., Barton E. D., Llinas O., 1985. The concentration of nutrient salts in "pure" North and South Atlantic Central Waters, in: *International Symposium on the most important Upwelling*

- Areas off Western Africa (Cape Blanc and Benguela)*, edited by C. Bas, R. Margalef and P. Rubies, Instituto de Investigaciones Pesqueras, Vol. I, Barcelona, 25-36.
- Gill A. E., Niiler P. P., 1973. The theory of seasonal variability in the ocean, *Deep-Sea Res.*, **20**, 141-177.
- Halpern D., Holbrook J. R., 1977. STD Measurements off Spanish Sahara, March/April 1974. CUEA (Coastal Upwelling Ecosystem Analysis) Data report 36, University of Washington, 1-15.
- Hickey B. M., 1979. The California current system. Hypotheses and facts, *Progr. Oceanogr.*, **8**, 191-279.
- Jones P. G. W., 1972. The variability of oceanographic observations off the coast of north-west Africa, *Deep-Sea Res.*, **19**, 405-431.
- Kirwan A. D., 1983. On "Oceanic Isopycnal Mixing by Coordinate Rotation", *J. Phys. Oceanogr.*, **13**, 1318-1319.
- Krauss W., Wuebber C., 1982. Response of the North Atlantic to annual wind variations along the eastern coast, *Deep-Sea Res.*, **29**, 851-868.
- Lass H. U., Wulff C., Schwabe R., 1983. Methoden und Programme zur automatischen Erkennung und Korrektur von Meßfehlern in ozeanologischen Vertikalprofilen, *Beitr. Meeresk.*, **48**, 95-111.
- Manriquez M., Fraga F., 1982. The distribution of water masses in the upwelling region off Northwest Africa in November. Rapp. P.-V. Réun. Cons. Int. Explor. Mer., Vol. 180, 39-47.
- Michelchen N., 1981. Estimates of large-scale atmospheric pressure variations in the upwelling area off Northwest Africa, in: *Coastal upwelling*, edited by F. A. Richards, AGU (American Geophysical Union), Washington, DC, 17-20.
- Mittelstaedt E., Pillsbury D., Smith R. L., 1975. Flow patterns in the northwest African upwelling area, *Disch. Hydrogr. Z.*, **28**, 145-167.
- Möckel F., 1980. Die ozeanologische Meßkette OM 75, eine universelle Datenerfassungsanlage für Forschungsschiffe, *Beitr. Meeresk.*, **43**, 5-14.
- Philander S. G. H., Yoon J. H., 1982. Eastern boundary currents and coastal upwelling, *J. Phys. Oceanogr.*, **12**, 862-879.
- Schemainda R., Nehring D., Schulz S., 1975. Ozeanologische Untersuchungen zum Produktionspotential der nordwestafrikanischen Wasserauftriebsregion 1970-1973. Geodätische und Geophysikalische Veröffentlichungen, Reihe IV, Heft 16, 85 p.
- Smed J., 1982. The oceanographic data base for the CINECA region, Rapp. P.-V. Réun. Cons. Int. Explor. Mer., Vol. 180, 11-28.
- Speth P., Detlefsen H., Sierts H. W., 1978. Meteorological influence on upwelling off Northwest Africa, *Disch. Hydrogr. Z.*, **31**, 95-104.
- Suginohara N., 1982. Coastal upwelling: onshore-offshore circulation, equatorward coastal jet and poleward undercurrent over a continental slope, *J. Phys. Oceanogr.*, **12**, 272-284.
- Sverdrup H. U., Johnson M. W., Fleming R. H., 1942. The water masses and currents of the oceans, in: *The oceans, their physics, chemistry and general biology*, Prentice-Hall, Inc., New York, 605-761.
- Tomczak M., 1978. De l'origine et la distribution de l'eau remontée à la surface au large de la côte nord-ouest africaine, *Anal. Hydrogr. Sér.*, **5**, 6, 5-14.
- Tomczak M., 1981 a. A multi-parameter extension of temperature/salinity diagram techniques for the analysis of non-isopycnal mixing, *Progr. Oceanogr.*, **10**, 147-171.
- Tomczak M., 1981 b. An analysis of mixing in the frontal zone of South and North Atlantic Central Water off North-West Africa, *Progr. Oceanogr.*, **10**, 3, 173-192.
- Tomczak M., Hughes P., 1980. Three dimensional variability of water masses and currents in the Canary Current upwelling region, "Meteor" *Forschungsergebn.*, **A**, **21**, 1-24.
- Veronis G., 1966. Rossby waves with bottom topography, *J. Mar. Res.*, **24**, 338-349.
- Verstraete J.-M., Picaut J., 1983. Variations du niveau de la mer, de la température de surface et des hauteurs dynamiques le long de la côte nord du Golfe de Guinée, *Oceanogr. Trop.*, **18**, 139-162.
- Willenbrink E., 1982. Wassermassenanalyse im tropischen und subtropischen Nordostatlantik, Berichte, Institut für Meereskunde, Universität Kiel, Nr. 96, 72 p.
- Wooster W. S., Bakun A., McLain D. R., 1976. The seasonal upwelling cycle along the eastern boundary of the North Atlantic, *J. Mar. Res.*, **34**, 2, 131-141.
- Yoshida K., 1967. Circulation in the eastern tropical oceans with special references to upwelling and undercurrents, *Jap. J. Geophys.*, **4**, 1-75.